

Effective moisture diffusivity and mathematical modeling of drying compost pellet

Ghafour Absalan, Mohammad Hossein Kianmehr^{*}, Akbar Arabhosseini

(Department of Agrotechnology, College of Abouraihan, University of Tehran, Tehran, Iran)

Abstract: Compost compression processes, such as pelleting, increase bulk density, improve storability, reduce transportation costs and make easier materials handling using existing equipment for handling and storage of grains. It is important to prevent quality deterioration of pellets in long time storage. Therefore, it is necessary to reduce the moisture content of the pellets to less than 20% or less. In this research the drying kinetics of compost pellets were studied at air temperatures of 50 °C, 60 °C and 70 °C, air velocities of 0.5, 1 and 1.5 m/s, particle sizes of 1.18 and 2 mm and pellet diameters of 6 and 8 mm. The maximum effective moisture diffusivity ($1.78 \times 10^{-9} \text{ m}^2/\text{s}$) was obtained at air velocity of 1.5 m/s, air temperature of 70 °C, particle size of 1.18 mm and pellet diameter of 8 mm. The activation energy of compost pellets varied from 25.88 to 57.4 kJ/mol under different conditions. The Page model was selected as the most suitable model, based on the statistical analysis.

Keywords: drying kinetics, effective moisture diffusivity, mathematical modeling, pellet

Citation: Absalan Gh, M. H. Kianmehr, and A. Arabhosseini. 2016 Effective moisture diffusivity and mathematical modeling of drying compost pellet. *Agricultural Engineering International: CIGR Journal*, 18 (2):156-169.

1 Introduction

Every day a huge amount of organic wastes generate by municipal, agricultural and agro-industrial activities and removal of the wastes causes energetic, economic and environmental problems (Castaldi and Melis 2002). In recent years, composting has become an interesting topic of the social demand for waste treatment technology and for organic agricultural products. Composting is a relevant method for waste treatment as a high level efficient method for waste disposal which enables recycling of organic matter (Greenway and Song 2002). Biomass materials, such as manures and farmyard compost from urban waste have high moisture content and high volume, which are non-uniform materials and cause limitation in usage of such materials. Densification, such as pelleting, is a solution for these problems which increase bulk density, improve storability, reduce

transportation costs, and make these materials easier to handle. In such conditions, the pellets become better suited and extremely cost effective to transport over long distances. In parallel, less storage space is required during the off season because of the high compactness of the pellets. The compost pellets can be applied by various kinds of existing machinery because of the uniform in size. They are also strong enough to transport and spread in the field by machine without disintegrating (Zafari and Kianmehr 2014). Deterioration of pellets during storage period is important in order to keep quality of the compost. More molds generate on the surface of compost pellets than ordinary compost with the same moisture content (Absalan et al., 2015). Deterioration is very noticeable, if mature composts are used to make the pellets. It is advised to reduce the moisture content of the pellets to less than 15%, because deterioration by condensation is caused even at 20% moisture content (Hara, 2001). Produced pellets were dried at ambient temperature until their moisture content reached about 12% (Zafari and Kianmehr 2012). Therefore, the compost pellets should be dried in a process to a relevant level of

Received date: 2016-01-08

Accepted date: 2016-04-03

*Corresponding author: Mohammad Hossein Kianmehr, Department of Agrotechnology, College of Abouraihan, University of Tehran, Tehran, Iran. Email: kianmehr@ut.ac.ir

moisture content. One of the most important aspects in drying technology is modelling of the drying process (Khazaei et al., 2008) and there has been some literature about drying and modeling drying of Biomass (Tumuluru et al., 2010; Chen et al., 2013; Yancey et al., 2013; Tumuluru, 2010). Physical and thermal properties of agricultural products such as heat and mass transfer, moisture diffusion and energy of activation are also required for ideal dryer design (Aghbashlo et al., 2008). The aim of this study was a) determination the effect of drying air velocity, air temperature, particle size and pellet diameter on dried compost pellets and b) evaluation of the fitting of the drying experimental data to five mathematical models available in the literature.

2 Materials and methods

2.1 Sample preparation for pelleting

Compost was obtained from composting laboratory in College of Abouraihan, University of Tehran and prepared for experiments. A chemical analysis of the compost was conducted by chemical analytical laboratory, University of Tehran (Table 1).

Table 1 Chemical analysis of the compost

Component	N, %	P, %	K, %	pH	CEC	EC
Content	2.3	0.54	1.6	7.4	125	1.57

The samples were screened through two sieves with sizes of 2 and 1.18 mm (meshes of 10 and 16, the American standard). Single screw extruder was used for producing the pellets the materials were compressed into the die installed at the end of the machine. Pellets with diameters of 6 and 8 mm were produced for each group of material size, which were sieved by different meshes. Initial moisture content of compost pellet was 46.21%.

2.2 Drying experiments

The drying experiments were performed at air temperatures of 50, 60 and 70°C and air velocities of 0.5, 1 and 1.5 m/s, then the effective moisture diffusivity, energy of activation of thin-layer drying pellet of compost were determined at each condition. The drying experiments were performed by using a laboratory scale batch dryer, developed at the Department of Agrotechnology, College of Abouraihan, University of Tehran (Figure 1).

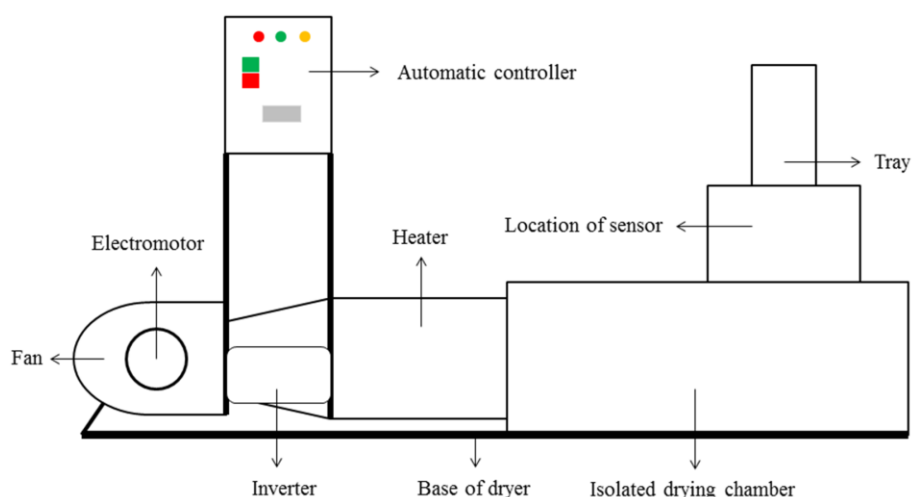


Figure 1 Laboratory scale of dryer, used for drying experiments

During the experiments, the ambient relative air humidity was about 40–50 % while the ambient air temperature was about 18–23°C. Hot air orientation to the samples was vertical (upward). In order to achieve a

desirable steady state condition, the dryer turned on about 20 min before each experiment. An inverter was fixed to control the air velocity through controlling the speed of the blower. An anemometer (PROVA AVM-07 model)

was used to regulate the required air velocity. Before each experiment, the samples were removed from the cold store and placed in a plastic bag in the laboratory to reach to the room temperature. Then, the pellets were spread in a thin layer (20 ± 0.1 mm) on the tray and placed in the dryer. The sample weight was measured and recorded every 10 minutes by using a digital balance with an accuracy of 0.01 g. The drying experiments continued until the mass between the two consecutive weighing was less than 0.05 g. After drying, the final moisture content of the samples were determined and considered as the equilibrium moisture content to calculate the moisture ratio (*MR*) Equation 1.

$$MR = \frac{M_t - M_e}{M_0 - M_e} \quad (1)$$

Where M_t is the moisture content (% d.b.), M_0 is the initial moisture content (% d.b.), and M_e is the equilibrium moisture content (% d.b.), of the sample or final moisture content in this research.

2.3 Determination of the effective diffusivity

Fick's second law of diffusion Equation (2) has been widely used to describe the drying process and interpret the experimental drying data during the falling rate period since internal mass transfer controls the drying process (Crank, 1975). The moisture diffusion is one of the main parameters that described this drying process so the Equation (2) can be used to interpret the experimental drying data (Celma et al., 2008; Chen et al., 2012). In this model the dependent variable is the moisture ratio (*MR*) which relates to the gradient of the sample moisture content at time t to both initial and equilibrium (final)

moisture content (Vega-Gálvez et al., 2010).

$$MR = \frac{M_t - M_e}{M_0 - M_e} = \frac{6}{\pi^2} \sum_{n=1}^{\infty} \frac{1}{n^2} \exp\left(-n^2 \pi^2 \frac{D_{eff} t}{r_0^2}\right) \quad (2)$$

The Equation (3) can be used at each constant drying temperature based on a constant moisture diffusivity assumption, which predicts a linear behavior between the mentioned variables (Doymaz, 2008; Chen et al., 2012).

As time increases, the terms other than the first approach are equal to zero. Neglecting higher terms of the equation:

$$MR = \frac{6}{\pi^2} \exp\left(-\pi^2 \frac{D_{eff} t}{r_0^2}\right) \quad (3)$$

The temperature dependence of the effective diffusivity can be represented by an Arrhenius relationship (Akgun and Doymaz, 2005) (See Equation (4)).

$$D_{eff} = D_0 \exp\left(-\frac{E_a}{R_g T_{abs}}\right) \quad (4)$$

Where R_g is the universal gas constant 8.214 kJ/mol, E_a is the activation energy, kJ/mol, D_0 is the Arrhenius factor, m^2/s and T_{abs} is the absolute temperature, K . Linear regression analyses were used to fit the equation to the experimental data to obtain correlation coefficient (R^2).

2.4 Mathematical modelling of the drying curves

The drying curves were fitted to five thin layer drying models, namely, Page, Newton, Henderson and Pabis, Logarithmic and Midilli-Kucuk (Table 2). The moisture ratio of compost pellet was calculated using the mathematical expression of Equation (2).

Table 2 Mathematical models selected to describe the pellet compost drying kinetics

No	Model Name	Model equation	Reference
1	Newton	$MR = \exp(-kt)$	Aghbashlo et al, 2009
2	Page	$MR = \exp(-kt^n)$	Diamante and Munro, 1993
3	Henderson and Pabis	$MR = a \exp(-kt)$	Zhang and Litchfield, 1991
4	Logarithmic	$MR = a \exp(-kt) + c$	Togrul and Pehlivan, 2002
5	Midilli-Kucuk	$MR = a \exp(-kt^n) + bt$	Midilli et al, 2002

2.4.1 Statistical evaluation of the models

The goodness of fit of the proposed models for simulating the drying kinetics data was evaluated by means of statistical tests including determination of correlation coefficient (R^2) Equation (5) chi-square (χ^2) Equation (6) and root mean square error (RMSE). Equation (7) (Aghbashlo et al., 2009). Models were fitted to experimental data by using MATLAB (v. R2013a) software.

$$R^2 = \frac{\sum_{i=1}^N (MR_{pre,i} - MR_{exp,i})^2}{\sum_{i=1}^N (MR_{exp,i} - MR_{exp,i})^2} \quad (5)$$

$$\chi^2 = \frac{\sum_{i=1}^N (MR_{exp,i} - MR_{pre,i})^2}{N - Z} \quad (6)$$

$$RMSE = \sqrt{\frac{1}{N} \sum_{i=1}^N ((MR_{pre,i}) - (MR_{exp,i}))^2} \quad (7)$$

Where $MR_{exp,i}$ is experimental moisture ratio, $MR_{pre,i}$ is predicted moisture ratio, N is the number of data values and Z is the number of parameters.

3 Results and discussion

The profiles of experimental moisture ratio as a function of time during drying of pellet compost samples at different air-drying temperatures are shown in Figure 2.

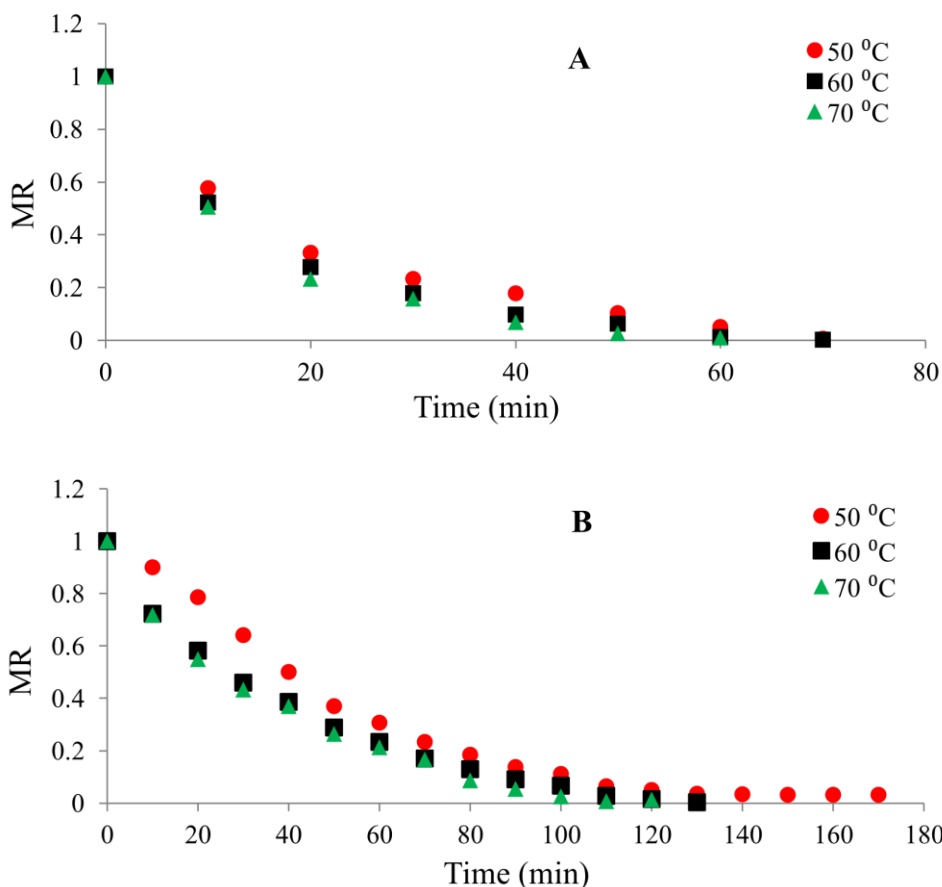


Figure 2 Moisture ratio of compost pellets during drying at different temperatures: a) air velocity of 1.5 m/s, particle size of 10 (2 mm) and diameter 6mm, b) air velocity of 0.5 m/s, particle size of 16 (1.18 mm), and diameter 8 mm.

The shortest drying time was for the pellets with particle size 16 and diameter of 6 mm while the longest drying time was for the pellets with the particle size 10 and

diameter of 8 mm. It can be seen that moisture ratio decreases continuously with increase temperature. In addition, drying rate is a function of drying air temperature,

diameter of pellet and particle size since at high temperature (e.g., 70°C) lower diameter (6 mm) and particle size (16 (1.18mm)) leads to shorter time to reach final moisture content. Similar effects of temperature on drying kinetics are reported for drying of other materials (Doymaz et al., 2004; Akgun and Doymaz 2005; Ghazanfari et al., 2006). Figure 3 shows the $\text{Ln}(MR)$ versus time (s) for drying of compost pellet. The figure shows that the drying of compost pellet occurred in falling rate period. The D_{eff} calculated using Equation (3) and varied in the range of 1.78×10^{-9} to 2.73×10^{-10} m²/s. The maximum value of D_{eff} was 1.78×10^{-9} m²/s at air

velocity of 1.5 m/s, air temperature of 70 °C, particle size of 16 (1.18 mm) and pellet diameter of 8 mm (Figure 3a). The D_{eff} values increased with increasing drying temperature, air velocity and diameter of pellet due to the increased surface area. More energy supply would increase the activity of water molecules when pellet of compost was dried at higher temperatures, leading to higher moisture diffusivity. The minimum value of D_{eff} was 2.73×10^{-10} m²/s at air velocity of 1 m/s and, air temperature of 50 °C, particle size of 16 (1.18 mm) and pellet diameter of 6 mm (Figure 3b).

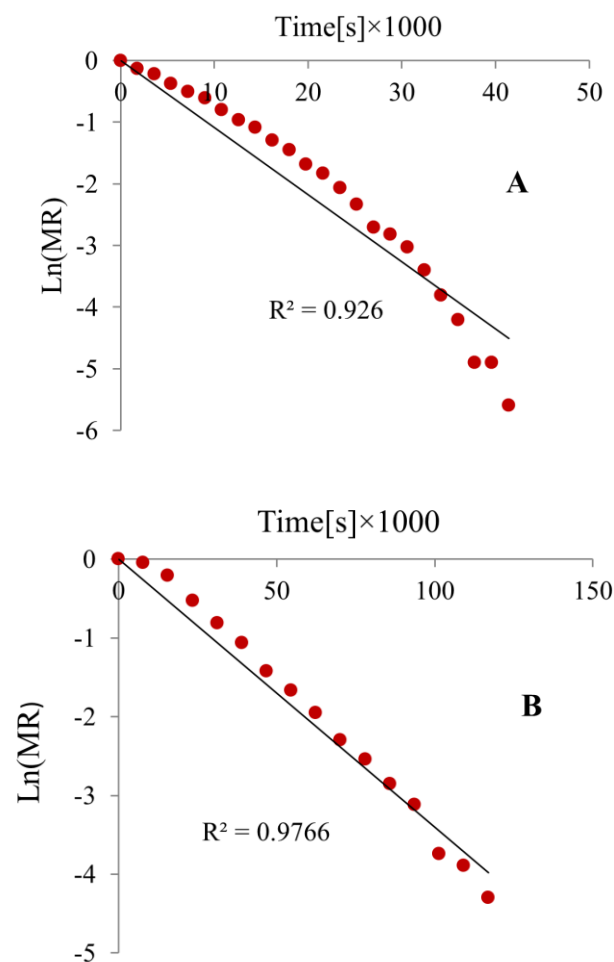


Figure 3 $\text{Ln}(MR)$ versus time (s) for thin-layer drying of compost pellet

The D_{eff} values obtained in this research were close to those reported for some other agricultural materials (Lopez et al., 2000; Montero et al., 2011). The value of $\text{Ln } D_{eff}$ versus $1/T_{abs}$ is shown in Figure 4. The energy of

activation (E_a) for compost pellet was calculated using Equation 4 which varied from 25.88 to 54.4 kJ/mol for different level of the examined parameters (air velocity, particle size and diameter of pellet). The maximum value

of E_a was 54.4 kJ/mol showing a linear relationship due to the Arrhenius-type dependence ($R^2 = 0.9981$) at air velocity of 0.5 m/s, particle size of 10(2 mm) and pellet diameter of 6 mm (Figure 4a) while the minimum value of

E_a was 25.88 kJ/mol, showing a linear relationship due to the Arrhenius-type dependence with high ($R^2 = 0.9452$) at air velocity of 0.5 m/s and the, particle size of 16(1.18 mm) and pellet diameter of 8 mm (Figure 4b).

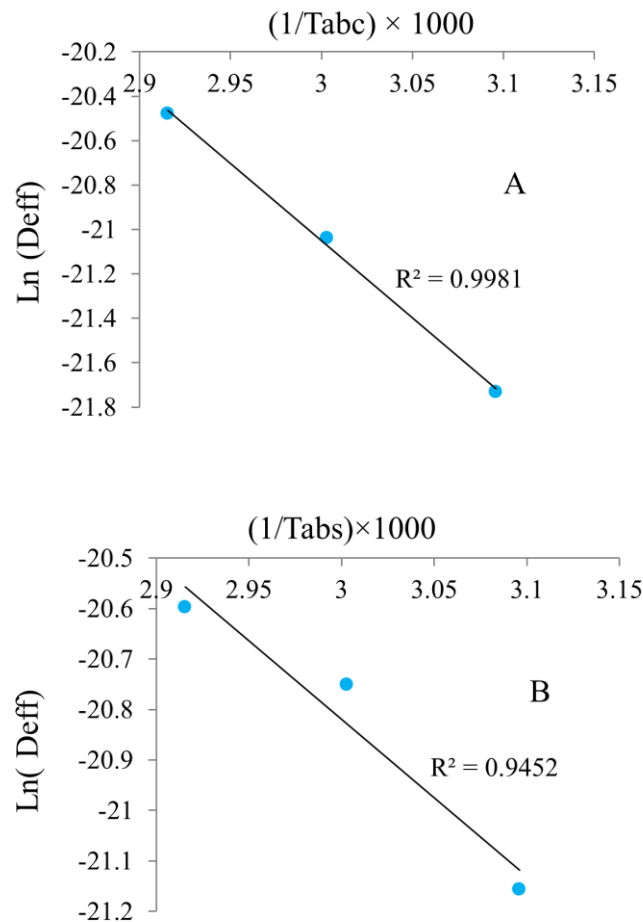


Figure 4 Correlation between effective moisture diffusivity and air temperature

The obtained values of moisture diffusivity for compost pellets were higher than some agricultural materials such as poplar sawdust: 12.3 kJ/mol (Chen et al., 2011), and for dry vegetable waste: 19.82 kJ/mol (Chong et al., 2008). The experimental data obtained in compost of pellet drying showed that the drying process occurs mainly in the falling rate period at all the process temperatures.

The experiential data were fitted to the five mathematical models in order to evaluate the one which is best for representing drying kinetics of pellets. The best model was chosen based on the highest R^2 , the least χ^2 and least $RMSE$. Lists the parameter values of the model and statistical analysis for each condition (from Tables 3 to Table 8).

Table 3 Statistical results of five mathematical models at different drying conditions for air velocities of 0.5 m/s and diameter 6 mm

Model	Temperature, °C	Model parameter				χ^2	RMSE	R ²
		a	b	K	n			
Mesh 16								
Page	50			0.0557	0.8859	0.0006	0.01404	0.9973
	60			0.0059	1.242	0.0007	0.01064	0.9988
	70			0.0634	0.9034	0.0000	0.009105	0.9990
Newton	50			0.0352		0.0008	0.01304	0.9975
	60			0.0174		0.0019	0.0291	0.9908
	70			0.0440		0.0002	0.00821	0.9992
Henderson and Pabis	50	0.848		0.0319		0.0008	0.01871	0.9949
	60	1.009		0.0178		0.0015	0.02983	0.9904
	70	0.9147		0.0418		0.0002	0.00979	0.9988
Logarithmic	50	0.9221	0.0095	0.0362		0.0008	0.04199	0.9744
	60	1.036	-0.0441	0.0157		0.0015	0.01879	0.9966
	70	0.9194	-0.0066	0.0407		0.0002	0.009737	0.9988
Midilli-Kucuk	50	0.933	-0.0001	0.0617	0.6933	0.0007	0.02697	0.9913
	60	0.9834	-0.0001	0.0122	1.068	0.0007	0.02167	0.9958
	70	0.987	-0.0001	0.0557	0.8859	0.0000	0.00610	0.9996
Mesh 10								
Newton	50			0.0096	1.182	0.0001	0.0114	0.9987
	60			0.0290	1.114	0.0000	0.0039	0.9998
	70			0.0369	1.183	0.0000	0.0079	0.9993
Page	50			0.0203		0.0007	0.0269	0.9924
	60			0.0427		0.0002	0.0127	0.9980
	70			0.0638		0.0006	0.0231	0.9940
Henderson and Pabis	50	1.23		0.0241		0.0006	0.0160	0.9973
	60	1.01		0.0433		0.0001	0.0122	0.9983
	70	1.03		0.0658		0.0005	0.0213	0.9952
Logarithmic	50	1.06	-0.041	0.0186		0.0060	0.0169	0.9973
	60	1.02	-0.008	0.0421		0.0001	0.0108	0.9988
	70	1.04	-0.020	0.0619		0.0005	0.0178	0.9965
Midilli-Kucuk	50	0.98	-0.000	0.0086	1.202	0.0066	0.0080	0.9994
	60	0.99	-0.000	0.0291	1.112	0.0003	0.0041	0.9998
	70	0.99	-0.000	0.0373	1.178	0.0000	0.0081	0.9994

Table 4 Statistical results of five mathematical models at different drying conditions for air velocities of 1 m/s and diameter 6 mm

Model	Temperature, °C	Model parameter				χ^2	RMSE	R ²
		a	b	k	n			
Mesh 16								
Page	50			0.0046	1.301	0.0005	0.0011	0.9988
	60			0.0273	1.042	0.0013	0.0068	0.9995
	70			0.0268	0.9536	0.0001	0.0395	0.9822
Newton	50			0.0188		0.0040	0.0226	0.9955
	60			0.0331		0.0014	0.0139	0.9979
	70			0.0221		0.0001	0.0389	0.9827
Henderson and Pabis	50	0.84		0.0020		0.0025	0.0207	0.9962
	60	1.00		0.0338		0.0013	0.0141	0.9978
	70	0.91		0.0216		0.0001	0.0427	0.9791
Logarithmic	50	0.92	-0.024	0.0188		0.0025	0.0251	0.9944
	60	1.03	-0.002	0.0335		0.0013	0.0148	0.9976
	70	0.91	-0.054	0.0184		0.0001	0.0359	0.9852
Midilli–Kucuk	50	0.93	-0.000	0.0026	1.435	0.0003	0.0212	0.9968
	60	0.98	-4.223	0.0327	1.006	0.0013	0.0159	0.9979
	70	0.98	-0.000	0.0493	0.7575	0.0001	0.0272	0.9932
Mesh 10								
Newton	50			0.0310	0.955	0.0007	0.02848	0.9901
	60			0.0118	1.337	0.0000	0.0098	0.9990
	70			0.0692	1.002	0.0002	0.01419	0.9976
Page	50			0.0252		0.0008	0.0028	0.9902
	60			0.0441		0.0009	0.0110	0.9987
	70			0.0696		0.0002	0.0137	0.9976
Henderson and Pabis	50	0.968		0.0252		0.0007	0.0275	0.9913
	60	1.53		0.0528		0.0006	0.0163	0.9973
	70	1.00		0.0697		0.0002	0.0141	0.9977
Logarithmic	50	0.983	-0.027	0.0231		0.0007	0.0253	0.9931
	60	1.52	-0.001	0.0524		0.0009	0.0185	0.9969
	70	1.00	-0.003	0.00313		0.0002	0.0144	0.9977
Midilli–Kucuk	50	0.985	-0.000	0.0395	0.870	0.0007	0.0230	0.9947
	60	1.00	-0.000	0.0113	1.352	0.0140	0.0106	0.9991
	70	1.00	-0.000	0.0720	0.986	0.0002	0.0148	0.9978

Table 5 Statistical results of five mathematical models at different drying conditions for air velocities of 1.5 m/s and diameter 6 mm

Model	Temperature, °C	Model parameter				χ^2	RMSE	R ²
		a	b	k	n			
Mesh 16								
Page	50			0.0338	0.946	0.0003	0.0181	0.9957
	60			0.0926	0.874	0.0002	0.0248	0.9923
	70			0.0475	1.091	0.0005	0.0102	0.9988
Newton	50			0.0281		0.0005	0.0214	0.9940
	60			0.0631		0.0003	0.0314	0.9870
	70			0.0657		0.0009	0.0191	0.9958
Henderson and Pabis	50	0.983		0.0276		0.0004	0.0216	0.9940
	60	0.949		0.0599		0.0003	0.0284	0.9900
	70	1.07		0.0685		0.0007	0.0169	0.9967
Logarithmic	50	0.983	0.000	0.0276		0.0004	0.0222	0.9936
	60	0.952	-0.006	0.0585		0.0003	0.0291	0.9901
	70	1.025	-0.009	0.0645		0.0007	0.0181	0.9967
Midilli–Kucuk	50	1.006	-0.000	0.0428	0.884	0.0003	0.0189	0.9962
	60	0.997	-0.000	0.1173	0.765	0.0002	0.0169	0.9969
	70	1.006	-0.000	0.0550	1.058	0.0005	0.0177	0.9971
Mesh 10								
Page	50			0.0606	0.926	0.0007	0.0061	0.999
	60			0.0471	1.063	0.0000	0.0081	0.9994
	70			0.1619	0.639	0.0000	0.0361	0.9837
Newton	50			0.0469		0.0013	0.0081	0.9992
	60			0.0574		0.0001	0.0104	0.9989
	70			0.0525		0.0001	0.0688	0.9372
Henderson and Pabis	50	0.988		0.0469		0.0012	0.0103	0.9988
	60	1.008		0.0578		0.0001	0.0106	0.9988
	70	0.8921		0.4368		0.0001	0.0831	0.9319
Logarithmic	50	0.9208	-0.001	0.0435		0.0011	0.0083	0.9991
	60	1.012	-0.006	0.0566		0.0001	0.01003	0.9990
	70	0.8889	-0.027	0.0511		0.0001	0.0636	0.9463
Midilli–Kucuk	50	0.9998	-0.000	0.0623	0.916	0.0015	0.0060	0.9996
	60	1.001	-0.000	0.0481	1.057	0.0000	0.0090	0.9994
	70	1.003	-0.000	0.187	0.582	0.0000	0.0353	0.9834

Table 6 Statistical results of five mathematical models at different drying conditions for air velocities of 0.5 m/s and diameter 8 mm

Model	Temperature, °C	Model parameter				χ^2	RMSE	R ²
		a	b	k	n			
Mesh 16								
Page	50			0.05244	0.8251	0.0001	0.00984	0.9993
	60			0.04398	0.9874	0.0006	0.0078	0.9975
	70			0.03476	1.042	0.0000	0.0029	0.9999
Newton	50			0.02534		0.0012	0.0083	0.9990
	60			0.03897		0.0018	0.0055	0.9942
	70			0.04119		0.0000	0.0059	0.9996
Henderson and Pabis	50	0.8089		0.02184		0.0009	0.0144	0.9969
	60	1.017		0.04335		0.0014	0.0122	0.9982
	70	0.9994		0.0412		0.0000	0.0063	0.9995
Logarithmic	50	0.9349	-0.017	0.02729		0.0008	0.0328	0.9841
	60	1.022	-0.008	0.04216		0.0014	0.0108	0.9988
	70	1.009	-0.004	0.04045		0.0000	0.0067	0.9995
Midilli–Kucuk	50	0.9981	-0.000	0.07984	0.7165	0.0001	0.0144	0.9969
	60	0.9988	-0.000	0.02912	1.112	0.0006	0.0041	0.9998
	70	1.002	-0.000	0.03827	1.018	0.0000	0.0067	0.9995
Mesh 10								
Page	50			0.0096	1.339	0.0001	0.0137	0.9983
	60			0.0092	1.233	0.0006	0.0129	0.9984
	70			0.0274	0.978	0.0005	0.0302	0.9900
Newton	50			0.0324		0.0021	0.0476	0.9786
	60			0.0234		0.0006	0.0350	0.9880
	70			0.0252		0.0005	0.0295	0.9899
Henderson and Pabis	50	1.085		0.0350		0.0013	0.0396	0.9852
	60	1.051		0.0245		0.0006	0.0319	0.9906
	70	0.9748		0.0246		0.0004	0.0293	0.9906
Logarithmic	50	1.122	-0.0560	0.0304		0.0013	0.0346	0.9887
	60	1.093	-0.0664	0.0205		0.0006	0.0176	0.9973
	70	0.9559	-0.0440	0.0215		0.0004	0.0241	0.9932
Midilli–Kucuk	50	1.002	0.0000	0.0082	1.392	0.0000	0.0107	0.9989
	60	0.966	-0.0001	0.0106	1.189	0.0006	0.0095	0.9993
	70	0.9889	-0.0004	0.0396	0.8544	0.0004	0.0205	0.9960

Table 7 Statistical results of five mathematical models at different drying conditions for air velocities of 1 m/s and diameter 8 mm

Model	Temperature, °C	Model parameter				χ^2	RMSE	R ²
		a	b	k	n			
Mesh 16								
Page	50			0.0321	0.968	0.0001	0.0125	0.9981
	60			0.0355	1.023	0.0001	0.0096	0.9991
	70			0.0022	1.085	0.0000	0.0272	0.9927
Newton	50			0.0284		0.0001	0.0130	0.9979
	60			0.0386		0.0002	0.0097	0.9990
	70			0.0314		0.0009	0.0301	0.9903
Henderson and Pabis	50	0.994		0.0283		0.0001	0.0133	0.9980
	60	1.002		0.0386		0.0001	0.00150	0.9988
	70	1.009		0.0313		0.0009	0.0311	0.9904
Logarithmic	50	0.997	-0.0038	0.0279		0.0001	0.0144	0.9978
	60	1.024	-0.0108	0.0372		0.0001	0.0127	0.9982
	70	1.02	-0.0190	0.0298		0.0009	0.0308	0.9898
Midilli–Kucuk	50	1.006	-0.0001	0.0370	0.925	0.0001	0.0111	0.9985
	60	1.005	0.0000	0.0308	1.059	0.0001	0.0015	0.9988
	70	1.011	-0.0002	0.0371	0.9449	0.0009	0.0312	0.9896
Mesh 10								
Page	50			0.0151	1.277	0.0001	0.01523	0.9979
	60			0.0523	0.999	0.0008	0.02398	0.9938
	70			0.0253	1.026	0.0002	0.02528	0.9933
Newton	50			0.0341		0.0011	0.0351	0.9879
	60			0.0522		0.0008	0.02322	0.9938
	70			0.0280		0.0012	0.02479	0.9931
Henderson and Pabis	50	1.055		0.0358		0.0009	0.03131	0.9910
	60	0.9855		0.0514		0.0007	0.02352	0.9941
	70	0.9962		0.0279		0.0007	0.02557	0.9926
Logarithmic	50	1.089	-0.055	0.0308		0.0009	0.0215	0.9955
	60	1.007	-0.036	0.0455		0.0007	0.01783	0.9968
	70	1.015	-0.033	0.0251		0.0009	0.02053	0.9958
Midilli–Kucuk	50	1.138	-0.000	0.0161	1.286	0.0001	0.01617	0.9979
	60	0.991	-0.000	0.0651	0.902	0.0007	0.01553	0.9978
	70	0.993	-0.000	0.0311	0.955	0.0002	0.02117	0.9959

Table 8 Statistical results of five mathematical models at different drying conditions for air velocities of 1.5 m/s and diameter 8 mm

Model	Temperature, °C	Model parameter				χ^2	RMSE	R ²
		a	b	k	n			
Mesh 16								
Page	50			0.0526	0.864	0.0001	0.0098	0.9989
	60			0.0759	0.890	0.0001	0.0135	0.9977
	70			0.0233	1.226	0.0001	0.0139	0.9980
Newton	50			0.0307		0.0005	0.0052	0.9997
	60			0.0522		0.0004	0.0191	0.9952
	70			0.0485		0.0012	0.0343	0.9873
Henderson and Pabis	50	1.00		0.0307		0.0004	0.0094	0.9989
	60	0.925		0.0504		0.0003	0.0078	0.9992
	70	1.054		0.0510		0.0009	0.0307	0.9898
Logarithmic	50	0.970	-0.0092	0.0325		0.0003	0.0202	0.9948
	60	0.962	-0.0006	0.0516		0.0003	0.01934	0.9951
	70	1.092	-0.0070	0.0427		0.0009	0.01714	0.9968
Midilli–Kucuk	50	0.979	-0.0000	0.0597	0.830	0.0001	0.00974	0.9990
	60	0.998	-0.0003	0.0857	0.84	0.0001	0.0087	0.9992
	70	0.982	-0.0002	0.0233	1.209	0.0001	0.00988	0.9989
Mesh 10								
Page	50			0.0258	1.176	0.0001	0.0181	0.9969
	60			0.0092	1.233	0.0002	0.0129	0.9983
	70			0.0253	1.026	0.0000	0.0252	0.9933
Newton	50			0.0463		0.0011	0.0311	0.9902
	60			0.0234		0.0008	0.0350	0.9880
	70			0.0492		0.0001	0.0105	0.9988
Henderson and Pabis	50	1.03		0.0478		0.0009	0.0297	0.9916
	60	1.05		0.0245		0.0007	0.0319	0.9906
	70	0.977		0.0492		0.0000	0.0109	0.9988
Logarithmic	50	1.081	-0.069	0.0397		0.0009	0.0130	0.9985
	60	1.093	-0.066	0.0205		0.0007	0.0176	0.9973
	70	1.017	-0.009	0.0479		0.0000	0.0082	0.9993
Midilli–Kucuk	50	1.00	-0.000	0.0342	1.07	0.0001	0.0012	0.9987
	60	0.996	-0.000	0.0106	1.189	0.0002	0.0095	0.9993
	70	0.999	-0.000	0.0385	1.072	0.0001	0.0055	0.9997

The Page models presented very good fits, however, the Page model contributed the best fitting with the highest R^2 and least χ^2 and least $RMSE$. Figure 5 illustrates the comparison of the experimental and predicted moisture

ratio values using this mathematical expression (Vega-Gálvez et al., 2010): These results clearly demonstrated that the Page model fits perfectly the drying kinetics of pellet of compost.

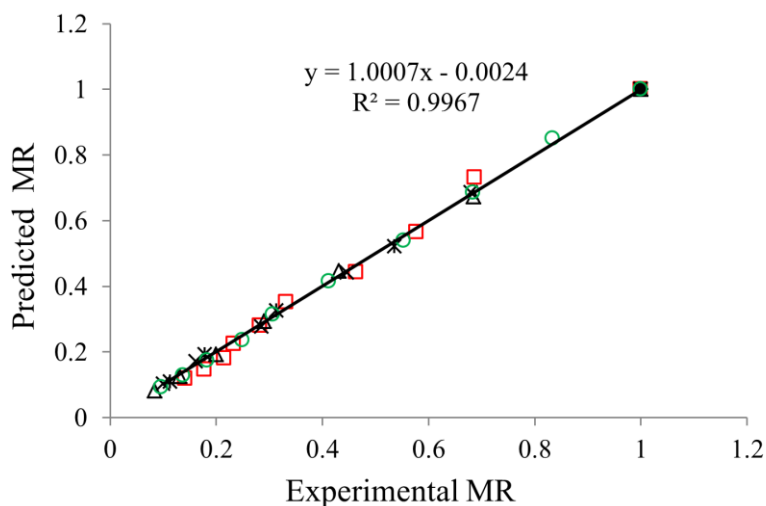


Figure 5 Experimental MR versus predicted MR by the Page model for pellet of compost

4 Conclusions

In this paper, the application of Arrhenius equation to experimental drying data is valid for the operation conditions employed in this investigation based on an assumption of diffusive controlling phenomenon allowed the estimation of moisture diffusivity as well as activation energy pellet of compost. The D_{eff} values increased with increasing drying temperature, air velocity and diameter of pellet due to the increased surface area. More energy supply would increase the activity of water molecules when pellet of compost was dried at higher temperatures, leading to higher moisture diffusivity. The obtained values of moisture diffusivity for compost pellets were higher than some agricultural materials such as poplar sawdust and dry vegetable waste. In order to explain the drying behavior of compost pellets, the experimental data were fitted to five different thin layer drying models and the models were compared according to their R^2 , $RMSE$ and χ^2 .

References

- Absalan Gh., M. H. Kianmehr, A. Arabhosseini, Sh. Kouravand. 2015. Optimization compressive strength biomass pellet from compost using Taguchi method. *Agricultural Engineering International: CIGR Journal*, 17(1):166-172.
- Aghbashlo M., M. H. Kianmehr, S. Khani, and M. Ghasemi. 2009. Mathematical modelling of thin-layer drying of carrot. *International Agrophysics*, 23(4): 313–317.
- Aghbashlo M., M. H. Kianmehr, and H. Samimi-Akhijahani. 2008. Influence of drying conditions on the effective moisture diffusivity, energy of activation and energy consumption during the thin-layer drying of berberis fruit (Berberidaceae). *Energy Conversion Management*, 49(10): 2865-2871.
- Akgun N., and I. Doymaz. 2005. Modelling of olive cake thin-layer drying process. *Journal of Food Engineering*, 68(4):455-461.
- Businelli M., R. Calandra, M. Pagliai, D. Businelli, G. Gigliotti, O. Grasselli, D. Said-Pullicino, and A. Leccese. 2007. Transformation of a landfill covering amended with municipal waste compost, Perugia, Italy. *Journal of Environment Quality*, 36(1):254–261.
- Castaldi P., and P. Melis. 2002. Composting of *Posidonioace anica* and its use in Agriculture. *Microbiology of composting*. Springer-Verlag, 425–434.
- Celma, A., F. Cuadros, and L. Rodriguez. 2008. Characterisation of industrial tomato by-products from infrared drying process. *Food and Bioproducts Processing*, 87(4), 282–291.
- Chen D., M. Li, and X. Zhu. 2013. Drying characteristics of powdered wheat straw and Its mathematical modeling. *Journal of Agricultural Science Technology*, 15(5): 869-877.
- Chen, D., Y. Zheng, and X. Zhu. 2012. Determination of effective moisture diffusivity and drying kinetics for poplar sawdust by thermo-gravimetric analysis under isothermal condition. *Bioresource Technology*, 107(1): 451–455.

- Chong, C. H., C. L. Law, M. Cloke, C. L. Hii, and L. C. Abdullah. 2008. Drying kinetics and product quality of dried Chempedak. *Journal of Food Engineering*, 88(4):522–527.
- Crank, J. 1975. *Mathematics of diffusion*. 2nd ed. London. Oxford University Press.
- Diamante, L. M., P. A. Munro. 1993. Mathematical modeling of thin layer solar drying of sweet potato slices. *Solar Energy*, 51(4): 271-276.
- Doymaz, I., O. Gorel, and N. A. Akgun. 2004. Drying characteristics of the solid by-product of olive oil extraction. *Biosystems Engineering*, 88(2): 213–219.
- Doymaz, I. 2005. Influence of pretreatment solution on the drying of sour-cherry. *Journal of Food Engineering*, 78(2): 591–596.
- Doymaz, I. 2008. Influence of blanching and slice thickness on drying characteristics of leek slices. *Journal of Food Engineering*, 47(1): 41–47.
- Ghazanfari, A., S. Emami, L. G. Tabil, and S. Panigrahi. 2006. Thin-Layer Drying of Flax Fiber: II. Modeling drying process using semi-theoretical and empirical models. *Drying Technology*, 24(12): 1637-1642.
- Greenway, G. M., and Q. J. Song. 2002. Heavy metal speciation in the composting process. *Journal of Environment Monitoring*, 4(2): 300–305.
- Hara, M. 2001. Fertilizer pellets made from composted livestock manure. *Food & Fertilizer Technology Center*, 1–12.
- Khazaei, J., G. R. Chegini, and M. Bakhshiani. 2008. Anovel alternative method for modeling the effects of air temperature and slice thickness on quality and drying kinetics of tomato slices: superposition technique. *Drying Technology*, 26(6): 759–775.
- Lopez A., A. Iguaz, A. Esnoz, P. Virseda. 2000. Thin layer drying behaviour of vegetable wastes from wholesale market. *Drying Technology*, 18(4-5): 995–1006.
- Midilli, A., H. Kucuk, and Z. Yapar. 2002. A new model for single layer drying. *Drying Technology*, 20(7): 1503–13.
- Montero, I. 2011. Thin layer drying kinetics of by-products from olive oil processing. *International Journal of Molecular Science*, 12(11): 7885–7897.
- Pietsch, W. 2002. *Agglomeration processes-phenomena, technologies, equipment*. Wiley-VCH.
- Tumuluru, J. S., L. G. Tabil, A. Opoku, M. R. Mosqueda, and O. Fadeyi. 2010. Effect of process variables on the quality characteristics of pelleted wheat distiller's dried grains with soluble. *Biosystems Engineering*, 105(4): 466-475.
- Togrul, I. T., and D. Pehlivan. 2002. Mathematical modelling of solar drying of apricots in thin layers. *Journal of Food Engineering*, 55(3): 209–216.
- Vega-Gálvez, A., M. Miranda, L. P. Díaz, L. Lopez, K. Rodriguez, and K. Di Scala. 2010. Effective moisture diffusivity determination and mathematical modelling of the drying curves of the olive-waste cake. *Bioresource Technology*, 101(19): 7265–7270.
- Yancey, N. A., J. S. Tumuluru, C. T. Wright. 2013. Drying, grinding and pelletization studies on raw and formulated biomass feedstock's for bioenergy applications. *Journal of Biobased Materials and Bioenergy*, 7(5): 549-558.
- Zafari, A., M. H. Kianmehr. 2014. Factors affecting mechanical properties of biomass pellet from compost. *Environmental Technology*, 35(4): 478-486.
- Zafari, A., M. H. Kianmehr. 2012. Effect of raw material properties and die geometry on the density of biomass pellets from composted municipal solid waste. *Bioresources*, 7(4): 4704-4714.
- Zhang, Q., and J. B. Litchfield. 1991. An optimization of intermittent corn drying in a laboratory scale thin layer dryer. *Drying Technology*, 9(2): 383–95.